http://dx.doi.org/10.5516/NET.02.2013.038

<Technical Note>

ELECTRICAL RESISTANCE IMAGING OF TWO-PHASE FLOW WITH A MESH GROUPING TECHNIQUE BASED ON PARTICLE SWARM OPTIMIZATION

BO AN LEE[1], BONG SEOK KIM[1], MIN SEOK KO[2], KYUNG YOUN KIM[3], and SIN KIM[1,2*]
[1]Institute for Nuclear Science and Technology, Jeju National University, Jeju 690-756, South Korea
[2]Department of Nuclear and Energy Engineering, Jeju National University, Jeju 690-756, South Korea
[3]Department of Electronic Engineering, Jeju National University, Jeju 690-756, South Korea
Corresponding author. E-mail : sinkim@jejunu.ac.kr

Received May 15, 2013
Accepted for Publication September 06, 2013

An electrical resistance tomography (ERT) technique combining the particle swarm optimization (PSO) algorithm with the Gauss-Newton method is applied to the visualization of two-phase flows. In the ERT, the electrical conductivity distribution, namely the conductivity values of pixels (numerical meshes) comprising the domain in the context of a numerical image reconstruction algorithm, is estimated with the known injected currents through the electrodes attached on the domain boundary and the measured potentials on those electrodes. In spite of many favorable characteristics of ERT such as no radiation, low cost, and high temporal resolution compared to other tomography techniques, one of the major drawbacks of ERT is low spatial resolution due to the inherent ill-posedness of conventional image reconstruction algorithms. In fact, the number of known data is much less than that of the unknowns (meshes). Recalling that binary mixtures like two-phase flows consist of only two substances with distinct electrical conductivities, this work adopts the PSO algorithm for mesh grouping to reduce the number of unknowns. In order to verify the enhanced performance of the proposed method, several numerical tests are performed. The comparison between the proposed algorithm and conventional Gauss-Newton method shows significant improvements in the quality of reconstructed images.

KEYWORDS : Electrical Resistance Tomography, Binary Mixture, Two-phase Flow, Mesh Grouping, Particle Swarm Optimization, Gauss-Newton Method

1. INTRODUCTION

Binary mixtures, like two-phase flow, are frequently encountered in various engineering systems. For example, in the chemical, oil, and nuclear industries, binary mixtures of chemical substances, oil-water, oil-air, steam-water are commonly observed in a single component. The information on the distribution of each substance is necessary in the design, the performance analysis, and the monitoring of the system. Especially, two-dimensional information on phase distribution in two-phase flow fields would be more favorable for theoretical model development and verification of CFD (Computational Fluid Dynamics) codes, since the two-phase flow phenomena are essentially multi-dimensional.

Many two-dimensional imaging methods like radiation absorption and scattering method [1], optical method [2], ultra sound method [3] and electrical methods [4] have been developed. Among these, electrical methods such as electrical resistance tomography (ERT) and electrical capacitance tomography (ECT) have favorable advantages, including no ionization radiation, low cost, and high temporal resolution compared to other methods. In this work, the electrical resistance tomography (ERT) technique is considered. The ERT uses the fact that the measured potentials on the electrodes attached on the domain boundary are dependent on the internal electrical conductivity distribution, or the phase distribution, for the given electrical currents through those electrodes. Based on the known injected currents and the measured potentials, the conductivity distribution is reconstructed with the aid of the ERT image reconstruction algorithm.

In the numerical algorithm, the problem domain is discretized into many small meshes (pixels) and each mesh is assumed to have a constant conductivity value. The phase distribution is approximated as the conductivity values of many meshes. The image reconstruction algorithm estimates the conductivity value in each mesh. The image reconstruction algorithm, so called the inverse algorithm, searches the optimal distribution of the conductivity values, minimizing the objective functional, that is the difference

between the measured potentials and the calculated potentials, by solving the governing equation with the assumed conductivity distribution and the boundary condition. In this, the potential distribution is computed numerically using usually the finite element method (FEM).

As the inverse algorithm to minimize the objective functional, the Gauss-Newton (GN) method is widely accepted [5]. However, the number of unknowns or meshes is much more than the number of current-potential data sets. Hence, the ERT image reconstruction is an inherently ill-posed problem. These characteristics result in low spatial resolution, which is the major drawback of the ERT.

For binary mixtures like two-phase flows in which there are only two distinct conductivity values, the number of unknowns can be reduced significantly and two approaches have been proposed. One is the mesh grouping approach and the other is the boundary estimation approach. The boundary estimation approach estimates the interface between the background and the secondary substances directly, not the conductivity distribution [6-11]. In this, the interfacial boundary should be properly parameterized with a few numbers of unknowns. Also, the mesh structure should be updated after each iteration step. In the mesh grouping approach, on the other hand, a number of meshes, which can be categorized into one of the substances, are grouped and each group is assumed to have a same conductivity value [4, 12-15]. As a result, the number of unknowns can be reduced significantly. Glidewell and Ng [12] proposed a two-step approach in electrical impedance imaging for medical tomography. In the first step, the anatomical information was obtained through the magnetic resonance imaging (MRI) data, and in the second step with this prior information, the internal configuration was preset and the meshes were grouped. Cho et al. [13] firstly introduced an adaptive mesh grouping algorithm to the ERT, in which the grouping criteria were determined by using the genetic algorithm and fuzzy set theory. Later, M.C. Kim et al. [14] employed the genetic algorithm only to determine the grouping criteria. K.Y. Kim et al. [15] suggested utilizing the predetermined threshold among the groups based on the best homogeneous resistivity value, and compared its performance with the grouping method based on the genetic algorithm. Recently, B.S. Kim et al. [16] applied the Otsu's method to select the optimal threshold.

This work proposes a new adaptive mesh grouping algorithm combining the particle swarm optimization (PSO) algorithm with the GN method for the improvement of spatial resolution. In this technique, the meshes are categorized into two groups: the background and the remnant groups. The PSO algorithm is used for the determination of the threshold between the groups and the representative conductivity value of the background group. Compared to the previous grouping algorithms like genetic algorithm and fuzzy set theory, the PSO, which is a recently developed evolutionary optimization algorithm, is easy to understand its concept and much simpler to implement, even with comparable optimization performance.

This paper consists of four parts. After the introduction, the 2nd section, the FEM formulation and the mathematical statement for the GN method are introduced. In the 3rd section, a mathematical demonstration for a proposed element grouping technique is described. In the 4th section, several numerical simulation results for the verification of the proposed algorithm are provided.

2. MATHEMATICAL MODEL

In general, the ERT is composed of the forward and the inverse problems. The process to obtain the potential distribution by solving the governing equation, subject to the given electrical conductivity values and boundary conditions, is called the forward problem, and the inverse problem is described as the process to estimate the internal conductivity distribution based on the measured voltages and the injected currents on the electrodes. A schematic flowchart is given in Fig. 1.

2.1 Forward Problem

When electrical currents I_ℓ are injected into the problem domain $\Omega \subset \Re^2$ through the ℓth electrode e_ℓ attached on the

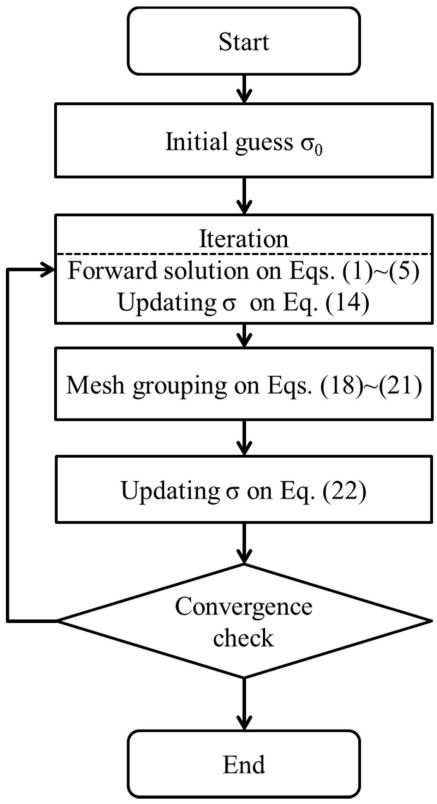

Fig. 1. Flowchart of Proposed Algorithm.

boundary $\partial\Omega$, and the conductivity distribution $\sigma(x, y)$ is known over the domain, the corresponding electrical potential $u(x, y)$ in Ω can be determined uniquely from the partial differential equation of the form:

$$\nabla\cdot(\sigma\nabla u)=0 \qquad \text{in } \Omega. \tag{1}$$

The boundary conditions are given by

$$\int_{e_\ell}\sigma\frac{\partial u}{\partial \nu}dS=I_\ell \qquad \text{on } e_\ell,\ \ell=1,2,\cdots,L, \tag{2}$$

$$\sigma\frac{\partial u}{\partial \nu}=0 \qquad \text{on } \partial\Omega_h, \tag{3}$$

$$u+z_\ell\sigma\frac{\partial u}{\partial \nu}=U_\ell \qquad \text{on } e_\ell,\ \ell=1,2,\cdots,L, \tag{4}$$

where $\partial\Omega=\sum_{\ell=1}^{L}e_\ell+\partial\Omega_h$ and L is the number of electrodes. The insulated boundary between electrodes is denoted by $\partial\Omega_h$. ν stands for the outward normal unit vector on the surface $\partial\Omega$, z_ℓ is the contact impedance, and U_ℓ is the measured boundary potential on the ℓ th electrode. Equation (4) is called the complete electrode model (CEM) which takes into account the discreteness and the shunting effect of the electrodes, and the contact impedance between the electrodes and the substance in Ω. In addition, the following two constraints for the injected currents and the measured electrode potentials should be imposed to ensure the existence and uniqueness of the solution:

$$\sum_{\ell=1}^{L}U_\ell=0 \ \text{ and } \ \sum_{\ell=1}^{L}I_\ell=0. \tag{5}$$

In this study, we use the finite element method (FEM) to obtain the numerical solution to the forward problem. In the context of FEM, the problem domain is discretized into sufficiently small triangular elements having a node at each corner, and it is assumed that the conductivity distribution is constant within each element [17]. The finite element formulation in a matrix form can be written as:

$$\mathbf{Ab}=\tilde{\mathbf{I}}, \tag{6}$$

where

$$\mathbf{A}=\begin{pmatrix}\mathbf{B} & \mathbf{CN}\\ (\mathbf{CN})^T & \mathbf{N}^T\mathbf{DN}\end{pmatrix},\ \mathbf{b}=\begin{pmatrix}\boldsymbol{\alpha}\\ \boldsymbol{\beta}\end{pmatrix}\ \text{and}\ \tilde{\mathbf{I}}=\begin{pmatrix}\mathbf{0}\\ \boldsymbol{\zeta}\end{pmatrix}. \tag{7}$$

In this, N is the number of nodes, $\boldsymbol{\alpha}=(\alpha_1, \alpha_2,\cdots, \alpha_N)^T\in\Re^{N\times1}$ is the voltage vector defined at the nodes, $\boldsymbol{\beta}=(\beta_1, \beta_2,\cdots, \beta_{L-1})^T\in\Re^{(L-1)\times1}$ is the reduced electrodes voltages, and $\mathbf{0}\in\Re^{N\times1}$. Here, the first constraint of (5) can be automatically satisfied by introducing the reduced voltage vector $\boldsymbol{\beta}$ and the mapping matrix $\mathbf{N}$

$$\mathbf{N}=\begin{pmatrix}1 & 1 & \cdots & 1\\ -1 & 0 & \cdots & 0\\ 0 & -1 & \cdots & 0\\ \vdots & \vdots & \ddots & \vdots\\ 0 & 0 & \cdots & -1\end{pmatrix}\in\Re^{L\times(L-1)} \tag{8}$$

instead of the electrode voltage vector $\mathbf{U}=(U_1, U_2,\cdots, U_L)^T=\mathbf{N}\boldsymbol{\beta}\in\Re^{L\times1}$. Also, $\boldsymbol{\zeta}=(I_1-I_2, I_1-I_3,\cdots, I_1-I_L)^T\in\Re^{(L-1)\times1}$ is the reduced current vector. The elements of stiffness matrix $\mathbf{A}$ are of the form

$$\mathbf{B}(i,j)=\int_\Omega\sigma\nabla\phi_i\cdot\nabla\phi_j d\Omega+\sum_{\ell=1}^{L}\frac{1}{z_\ell}\int_{e_\ell}\phi_i\phi_j dS,\ \ i,j=1,2,\cdots,N, \tag{9}$$

$$\mathbf{C}(i,j)=-\frac{1}{z_j}\int_{e_j}\phi_i dS,\quad i=1,2,\cdots,N,\ \ j=1,2,\cdots,L, \tag{10}$$

$$\mathbf{D}(i,j)=\begin{cases}0 & i\neq j\\ \dfrac{|e_j|}{z_j} & i=j\end{cases},\qquad i,j=1,2,\cdots,L, \tag{11}$$

where ϕ is the two-dimensional first order basis function and $|e_j|$ is the area of the electrode e_j.

2.2 Inverse Problem

Generally, the image reconstruction in the ERT becomes a problem of finding σ that minimizes the objective functional defined as:

$$\Phi(\sigma)=\frac{1}{2}\left[V-U(\sigma)\right]^T\left[V-U(\sigma)\right], \tag{12}$$

where V is the measured potential and is the calculated potential with the assumed σ.

Due to the ill-conditioning of the ERT inverse problem, regularization is usually introduced and the objective functional to be minimized is modified as

$$\Phi(\sigma)=\frac{1}{2}\left[V-U(\sigma)\right]^T\left[V-U(\sigma)\right]+\frac{\lambda}{2}\left[R(\sigma-\sigma^*)\right]^T\left[R(\sigma-\sigma^*)\right], \tag{13}$$

where R is the regularization matrix, λ is the regularization parameter, and σ^* is the prior information on the conductivity vector [14].

In this work, we employ the implicitly scaled Levenberg-Marquardt regularization scheme as the regularization method[18], and set the prior information to the conductivity at the previous iteration step since no prior is available. Hence, the iterative equation for updating the conductivity vector is derived as

$$\Delta\sigma^i=\sigma^{i+1}-\sigma^i=\left[J^TJ+\lambda\,\mathrm{diag}(J^TJ)\right]^{-1}J^T\left[V-U(\sigma^i)\right], \tag{14}$$

where $\sigma^i\in\Re^{E\times1}$ is the conductivity vector at the ith iteration and E is the number of elements. The Jacobian matrix $J\in\Re^{L\times E}$ is defined as

$$J_{ij}=\frac{\partial U_j}{\partial\sigma_i},\qquad i=1,2,\cdots,E \ \text{ and } \ j=1,2,\cdots,L. \tag{15}$$

3. ELEMENT GROUPING TECHNIQUE BASED ON PSO

The conventional GN algorithm is widely accepted as an inverse algorithm in the ERT, due to its robustness and relatively good performance. Even with a few iterations it can reconstruct the outline of the conductivity distribution. However, the objective functional tends not to be minimized further with more iterations and the spatial resolution is improved no more. This is one of the major drawbacks in the conventional inverse algorithms and results in poor spatial resolution in reconstructed images.

In order to improve the spatial resolution, this work introduces a mesh grouping approach. The mesh grouping can be a useful approach, especially when the ERT is applied to the domain composed of two substances with distinct conductivity values, like two-phase flows. During the iterations for the image reconstruction, by grouping the meshes that can be categorized as the same substance (background fluid or secondary fluid), the number of meshes reduces substantially and the reconstruction performance can be enhanced. There have been several strategies to categorize the meshes, as reviewed in Section 1. This work adopts the particle swam optimization (PSO) algorithm. This is applied after a few iterations with the GN algorithm, since for the first several iterations the GN shows a good performance.

The PSO algorithm is a computational method for optimization, by simulating the social behavior of bird flocking and their means of information exchange to search for their destination (optimal solution) [19]. In the PSO, a population of birds (particles) with random information (solutions) is initially guessed. Then, each particle moves through the solution space with a random velocity. The particle is guided to its best solution so far, and at the same time to the global best solution of the whole population so far. This process is repeated until the solution is sufficiently optimized.

This algorithm can be described as follows:

$$v_{k+1} = a \otimes v_k + b_1 \otimes w_1 \otimes \left(p_{Lbest} - x_k \right) + b_2 \otimes w_2 \otimes \left(p_{Gbest} - x_k \right), \quad (16)$$

$$x_{k+1} = x_k + v_{k+1}, \quad (17)$$

where $v_k \in \Re^{n \times 1}$ is the velocity vector and $x_k \in \Re^{n \times 1}$ the solution vector when n is the number of particles. The symbol $\otimes$ denotes element-by-element vector multiplication. w_1 and w_2 are the random numbers usually uniformly selected in the range [0, 1]. At the iteration step $k + 1$, the velocity v_{k+1} is updated on the basis of the current velocity weighted by a momentum factor a, the strength of the attraction to the local best solution of the current particle (P_{Lbest}), and to the global best solution in the whole population (P_{Gbest}) by the coefficient b_1 and b_2. The performance of the PSO is affected by the selection of the parameters a, b_1 and b_2. Trelea [20] derived a graphical parameter selection guideline and recommended a = 0.6 and $b_1 = b_2 = b = 1.7$.

The conceptual basis for image reconstruction with the mesh grouping using the PSO algorithm is summarized in Fig. 2. Figures 2(a) and (b) show a typical reconstructed image and the sorted conductivity curve in ascending order from the GN method, respectively. It is assumed that the background substance is much more conductive than the secondary substance. Ideally, the sorted conductivity profile should look like a step, since there are only two distinct conductivity values. At least, the profile should have two plateaus representing two substances and a connecting region with the conductivity values between the two, due to the interface-crossing meshes in the sense of the numerical analysis. In practice, as can be seen in Fig. 2(b) however, we cannot expect to get a well-distinguished conductivity profile, since the inverse estimation will not be perfect and there are always meshes crossing the interface between two substances.

In the mesh grouping, the conductivity values like Fig. 2(b) are classified into two different representative groups, i.e. the background and the secondary groups, and a representative conductivity value of each group is determined. Let $\bar{\sigma}_i$ (i = 1, 2) be the averaged values of each group and m be the boundary index between the groups. Then, we can formulate the following optimization problem to determine $\bar{\sigma}_i$ and m.

Find

$$\mathbf{X} = \left(\bar{\sigma}_1, \bar{\sigma}_2, m \right) \quad (18)$$

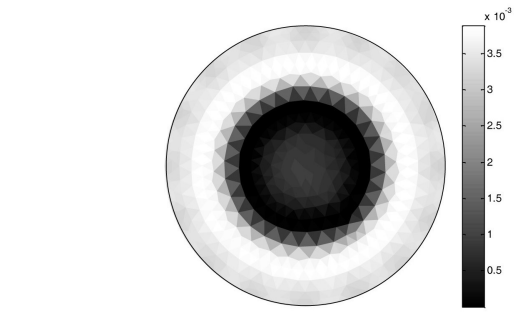

(a)

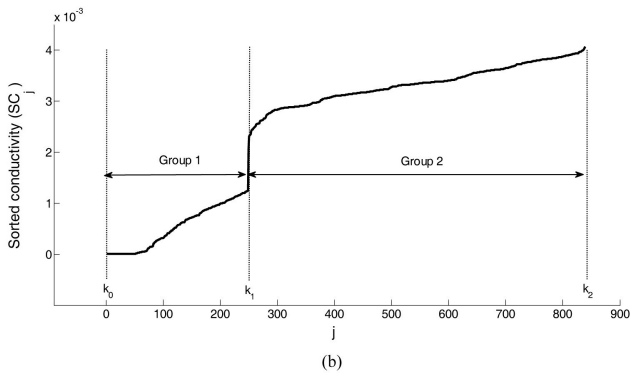

(b)

Fig. 2. Results for Conventional Reconstruction Algorithm: (a) Reconstructed Conductivity Distribution and (b) Conductivity Distribution in Ascending Order Obtained after 30 Iterations with GN Algorithm.

to minimize

$$f(\mathbf{X}) = \sum_{j=1}^{m} \left(\tilde{\sigma}_j - \bar{\sigma}_1\right)^2 + \sum_{j=m+1}^{E} \left(\tilde{\sigma}_j - \bar{\sigma}_2\right)^2 \quad (19)$$

where, $\mathbf{X}$ is the candidate solution, $\tilde{\sigma}_j (\tilde{\sigma}_j \le \tilde{\sigma}_{j+1}, J=1, 2\cdots, E-1)$is the sorted conductivity values in ascending order, and E is the total number of meshes (or unknown conductivity values). The optimization problem of Eq. (19) is solved by the PSO algorithm. In this study, we divide the groups into two groups, namely the background group (BG) and the remnant group (RG), which may include the meshes corresponding to the secondary fluid and the meshes crossing the interface. After the mesh grouping, the Jacobian matrix for the grouped meshes is modified as the following equation:

$$J_G = JG \in \Re^{L\times(m+1)}, \quad (20)$$

where G is the grouping matrix. The grouping matrix is obtained by

$$G = \left[G_{RG}\ G_{BG}\right], \quad (21)$$

where the $G_{RG} \in \Re^{E\times m}$ matrix extracts the meshes belonging to the RG, and the location of the meshes when their conductivity values are sorted in ascending order within the RG. $G_{BG} \in \Re^{E\times 1}$ is the vector of the meshes belonging to the BG, and the meshes of the BG are regarded as a single mesh with the same conductivity during the iteration. Hence, the number of unknowns is reduced from E to $m + 1$.

Once the grouping is applied, the meshes are rearranged and grouped, and then the conductivity increment of the grouped meshes should be modified as:

$$\Delta\sigma_G^i = \left[J_G^T J_G + \lambda \mathrm{diag}\left(J_G^T J_G\right)\right]^{-1} J_G^T \left[V - U(\sigma^i)\right]. \quad (22)$$

In the mesh grouping, as pointed out by Cho et al. [13], once the meshes are grouped improperly, the reconstruction performance may be deteriorated inadvertently. To remedy this wrong grouping, they suggested using the GN only without grouping after a certain number of iterations with the grouped meshes. In doing so, improperly grouped meshes can escape from the wrong group and acquire a chance to alter their conductivity values toward the minimization of the objective functional.

4. NUMERICAL EXPERIMENTS

In numerical experiments, two different meshes were used for the prevention of the inverse crime, as shown in Fig. 3 [21]. If the same mesh structure is used for the generation of the simulated measurement data and the image reconstruction, the reconstruction error may be canceled out unintentionally. A mesh structure with 2002 elements for the forward problem and another mesh structure with 840 elements for the inverse problem were used, respectively. For numerical simulations, a circular pipe with a 4 cm radius was considered. It was assumed that 16 electrodes with 0.6 cm width were installed evenly on the boundary, and these were illustrated as bold lines in Fig. 3. Two adjacent electrodes were selected as a source and a sink, while others were insulated. This current injection protocol was applied sequentially. The magnitude was 10 mA.

For the verification of the performance of the proposed algorithm, it was compared with the conventional GN method without grouping for 4 different two-phase flows, which could occur in horizontal pipes. The PSO was applied after 5 GN iterations without the mesh grouping, and to prevent improper grouping, after every 5 iterations the GN was solely applied without grouping.

In order to quantitatively investigate the estimation performance, the following root-mean-square error was introduced.

$$\mathrm{RMSE}_{cond} = \sqrt{\frac{\left(\sigma_{true} - \sigma_{est}\right)^T \left(\sigma_{true} - \sigma_{est}\right)}{\sigma_{true}^T \sigma_{true}}} \quad (23)$$

where σ_{true} and σ_{est} were the original conductivity vector and estimated conductivity vector, respectively.

As the first scenario, a two-phase stratified flow was considered. Figure 4(a) shows the true conductivity distribution for the stratified flow, and Figs. 4(b) and (c) indicate the reconstructed conductivity distributions by the conventional GN method only, and by the proposed method

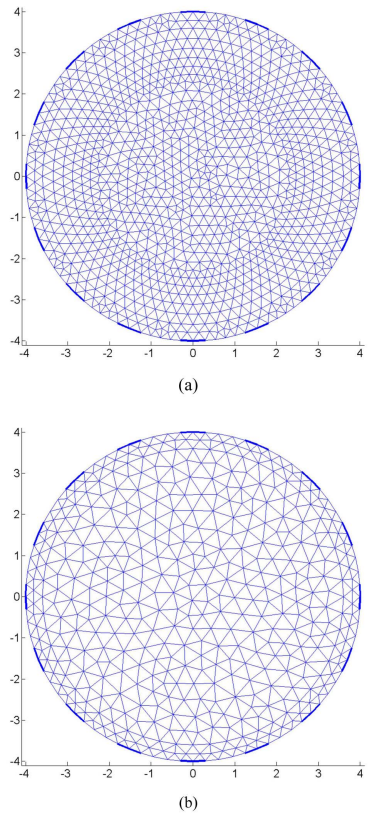

Fig. 3. Mesh Structures for (a) Forward Solver and (b) Inverse Solver.

combining the GN and the PSO method, respectively. The comparison between two different methods implies that the reconstruction performance of the proposed method is much better than the conventional GN method in terms of the image quality. Also, as can be seen in Fig. 5, the corresponding RMSE values support this numerical trend (0.38 for the GN method, 0.25 for the proposed method after 35 iterations). According to Figs. 6 and 7, for a wavy interface case, the proposed method still shows a much better performance. For a distorted gas core case, as given

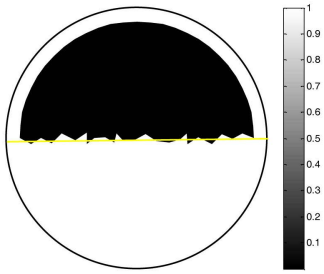

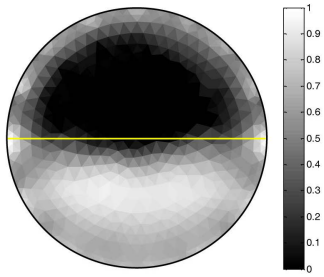

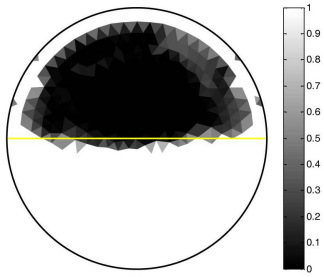

Fig. 4. Stratified Interface in the Domain: (a) True, (b) GN Only and (c) GN with Element Grouping Method.

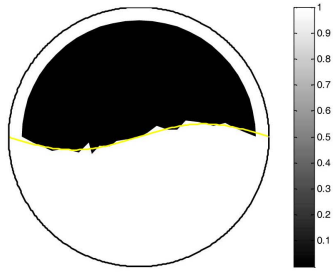

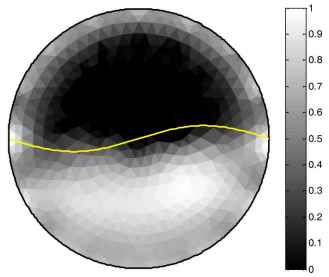

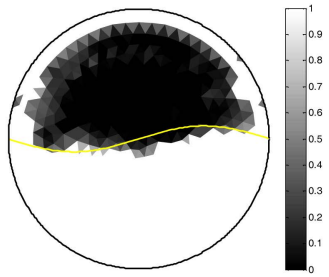

Fig. 6. Wavy Interface in the Domain: (a) True, (b) GN Only and (c) GN with Element Grouping Method.

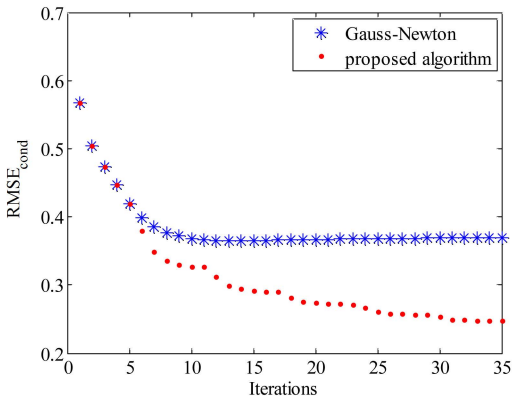

Fig. 5. The RMSE Values from the Conventional GN and the Proposed Algorithm for the Stratified Interface.

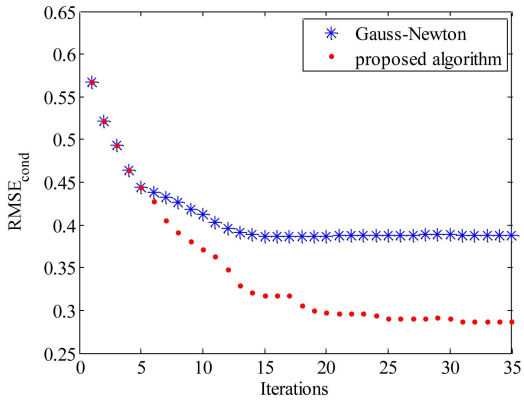

Fig. 7. The RMSE Values from the Conventional GN and the Proposed Algorithm for Wavy Interface.

in Figs. 8 and 9, and for an elongated bubble case as given in Figs. 10 and 11, the proposed method successfully differentiates the boundary of the air/vapor region from the background medium, while the conventional GN method gives the rough shapes for both cases.

5. CONCLUSIONS

We introduced a new image reconstruction algorithm combining the GN method with the PSO algorithm for the visualization of two-phase flows. For the verification

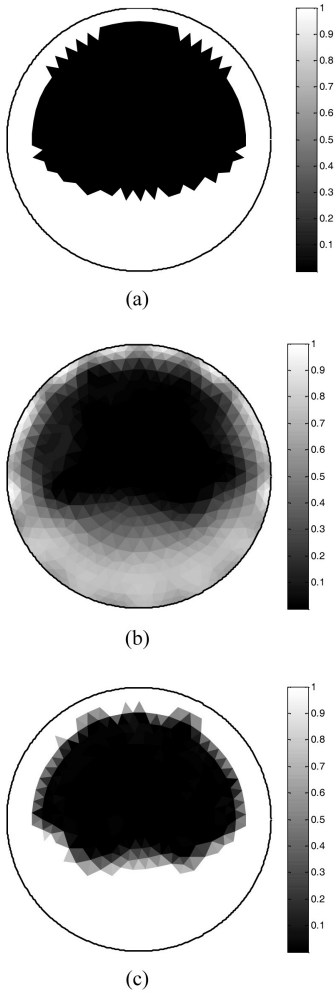

Fig. 8. Distorted Gas Core in the Domain: (a) True, (b) GN Only and (c) GN with Element Grouping Method.

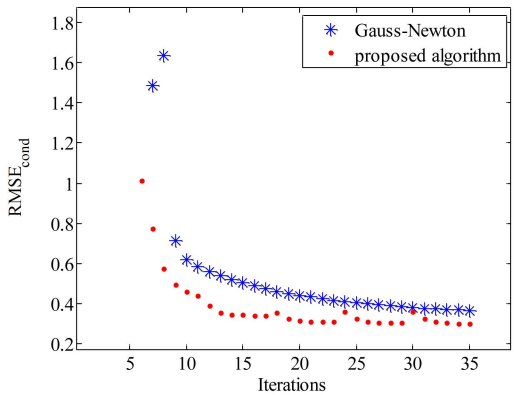

Fig. 9. The RMSE Values from the Conventional GN and the Proposed Algorithm for Distorted Gas Core.

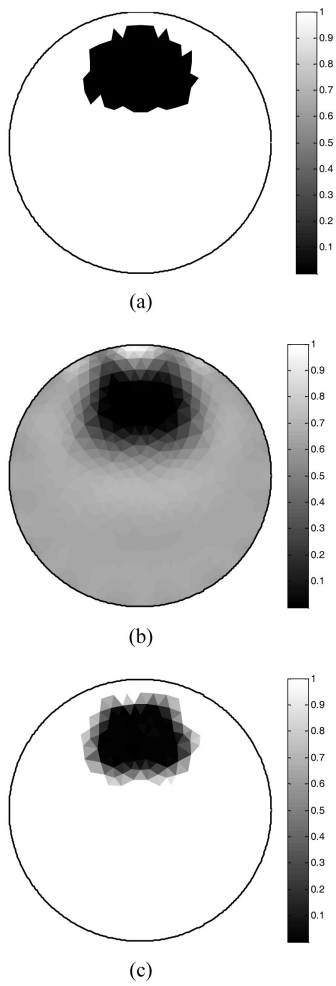

Fig. 10. Elongated Bubble in the Domain: (a) True, (b) GN Only and (c) GN with Element Grouping Method.

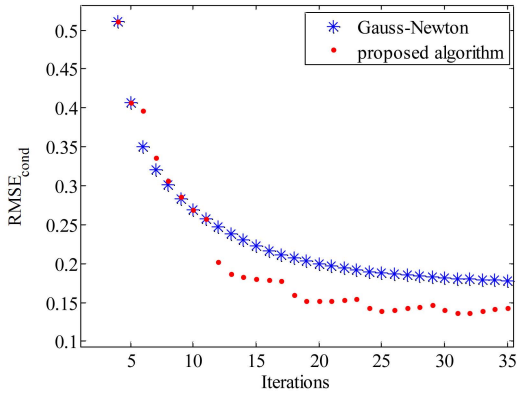

Fig. 11. The RMSE Values from the Conventional GN and the Proposed Algorithm for Elongated Bubble.

of the performance of the proposed technique several numerical experiments were conducted. In numerical tests, the proposed one was compared to the conventional GN algorithm. The comparison showed that the proposed technique significantly improved the image reconstruction performance.

ACKNOWLEDGMENTS

This work was done while the author his research year Jeju National University in 2012.

NOMENCLATURE

$\mathbf{A}$	Stiffness matrix
E	Number of elements
G	Grouping matrix
I	Electrical current
J	Jacobian matrix
L	Number of electrodes
N	Number of nodes
$\boldsymbol{N}$	Mapping matrix
R	Regularization matrix
U	Boundary potential
V	Measured potential
$\mathbf{X}$	Candidate solution
u	Electrical potential
z	Contact impedance

Greek Letters

σ	Conductivity distribution
Ω	Problem domain
$\boldsymbol{\alpha}$	Voltage vector defined at the nodes
$\boldsymbol{\beta}$	Reduced voltage vector
ζ	Reduced current vector
ϕ	Two-dimensional first order basis function
Φ	Objective function
λ	Regularization parameter
σ^*	Prior information on the conductivity vector
v_k	Velocity vector
x_k	Solution vector
$\tilde{\sigma}_j$	Sorted conductivity values
σ_{true}	Original conductivity vector
σ_{est}	Estimated conductivity vector

REFERENCES

[1] M. Bieberle, F. Barthel, and U. Hampel, "Ultrafast X-ray computed tomography for the analysis of gas-solid fluidized beds," *Chem. Eng. J*., vol. 189-190, pp. 356-363 (2012).

[2] P. F. Vassallo, T. A. Trabold, W. E. Moore, and G. J. Kirouac, "Measurement of velocities in gas-liquid two-phase flow using laser Doppler velocimetry," *Exp. Fluids*., vol. 15, pp. 227-230 (1993).

[3] L. Xu, Y. Han, L. A. Xu, and J. Yang, "Application of ultrasonic tomography to monitoring gas/liquid flow," *Chem. Eng. Sci*., vol. 52, pp. 2171-83 (1997).

[4] F. Dickin and M. Yang, "Electrical resistance tomography for process application," *Meas. Sci. Technol*., vol. 7, pp. 247-260 (1996).

[5] T. J. Yorkey, J. G. Webster, and W. J. Tompkins, "Comparing reconstruction algorithms for electrical impedance tomography," *IEEE T. Bio-med. Eng*., vol. 34, pp. 843-852 (1986).

[6] D. K. Han and A. Prosperetti, "A shape decomposition technique in electrical impedance tomography," *J. Comput. Phys*., vol. 155, pp. 75-95 (1999).

[7] V. Kolehmainen, S. R. Arridge, W. R. B. Lionheart, M. Vauhkonen, and J. P. Kaipio, "Recovery of region boundaries of piecewise constant coefficients of an elliptic PDE from boundary data," *Inverse Probl*., vol. 15, pp. 1375-1391 (1999).

[8] E. T. Chung, T. F. Chan, and X. C. Tai, "Electrical impedance tomography using level set representation and total variational regularization," *J. Comput. Phys*., vol. 205, pp. 357-372 (2005).

[9] B. Kortschak and B. Brandstätter, "A FEM-BEM approach using level-sets in electrical capacitance tomography," *COMPEL*, vol. 24, pp. 591-605 (2005).

[10] U. Z. Ijaz, A. K. Khambampati, J. S. Lee, S. Kim, and K. Y. Kim, "Nonstationary phase boundary estimation in electrical impedance tomography using unscented Kalman filter," *J. Comput. Phys*., vol. 227, pp. 7089-7112 (2008).

[11] A. K. Khambampati, U. Z. Ijaz, J. S. Lee, S. Kim, and K. Y. Kim, "Phase boundary estimation in electrical impedance tomography using the Hooke and Jeeves pattern search method," *Meas. Sci. Technol*., vol. 21, pp. 1-13 (2010).

[12] M. Glidewell and K. T. Ng, "Anatomically constrained electrical impedance tomography for anisotropic bodies via a two-step approach," *IEEE T. Med. Imaging*, vol. 14, pp. 498-503 (1995).

[13] K. H. Cho, S. Kim, and Y. J. Lee, "Impedance imaging of two-phase flow field with mesh grouping method," *Nucl. Eng. Des*., vol. 204, pp. 57-67 (2001).

[14] M. C. Kim, S. Kim, K. J. Lee, K. Y. Kim, "Improvement of the electrical impedance tomographic image for the two-phase system with adaptive element grouping technique," *Meas. Sci. Technol*., vol. 15, pp. 1391-1401 (2004).

[15] K. Y. Kim, B. S. Kim, M. C. Kim, S. Kim, Y. J. Lee, H. J. Jeon, B. Y. Choi, and M. Vauhkonen, "Electrical Impedance Imaging of Two-Phase Fields With an Adaptive Mesh Grouping Scheme," *IEEE T. Magn*., vol. 40, pp. 1124-7 (2004).

[16] B. S. Kim, A. K. Khambampati, S. Kim, and K. Y. Kim, "Image reconstruction with an adaptive threshold technique in electrical resistance tomography," *Meas. Sci. Technol*., vol. 22 (2011).

[17] M. Vauhkonen, "Electrical impedance tomography and prior information" [dissertation]. Kuopio, University of Kuopio (1997).

[18] M. C. Kim, S. Kim, K. Y. Kim, and Y. J. Lee, "Regularization methods in electrical impedance tomography technique for the two-phase flow visualization," Int. Comm. Heat Mass Transfer, vol. 28, pp. 773-782 (2004).

[19] J. Kennedy and R. C. Eberhart, "Particle swarm optimization," *In: Proceedings of IEEE International Conference on Neural Networks*, Piscataway: NJ (1995).

[20] I. C. Trelea, "The particle swarm optimization algorithm: convergence analysis and parameter selection," *Inform. Process Lett*., vol. 85, pp. 317-325 (2003).

[21] W. R. B. Lionheart, "EIT reconstruction algorithms: pitfalls, challenges and recent developments," *Physiol. Meas*., vol. 25, pp. 125-142 (2004).